Elastic Proton-Proton Collisions at 6.2 Bev in Nuclear Emulsions*

R. M. KALBACH,† J. J. LORD, AND C. H. TSAO
University of Washington, Seattle, Washington
(Received September 8, 1958)

Ilford G-5 emulsions were exposed to the 6.2-Bev proton beam of the Berkeley Bevatron. Of the interactions located, 31 could be classified as elastic collisions of beam protons with free, hydrogen nuclei. After correction for scanning efficiency and background events, an elastic scattering cross section of 8.8 ± 2.0 mb was obtained. The center-of-mass system angular distribution of elastically scattered protons is sharply peaked in the forward and backward direction and is in fair agreement with the prediction of a uniform optical model with a radius of 0.94×10^{-13} cm, a phase shift of 0.00 radian, and an opacity of 0.81. The results are compared with those of previous experiments.

I. INTRODUCTION

THE purpose of this paper is to present evidence relating to the nature of elastic proton-proton scattering at a bombarding energy of 6.2 Bev in nuclear emulsions, thereby affording a basis for speculation on the structure of the proton at this energy. The methods employed in this experiment were designed to permit examination of both elastic and inelastic processes at this energy. Data relating to collisions in which mesons are produced will be given in the following paper.

A complete quantum mechanical description of the elastic scattering process at such a high bombarding energy will contain a large number of undetermined parameters, since a phase shift must be assigned to each angular momentum state which participates in the interaction. In order to account for the observed meson production, such phase shifts must be considered as complex quantities, the real and imaginary parts corresponding to refraction and absorption, respectively, of the incident partial waves.

Experimental scattering data generally yields the elastic and inelastic cross sections together with an angular distribution of the scattered particles. If these data were given with sufficient precision, it would be possible to determine the various complex phase shifts with little ambiguity. However, such assignments become quite arbitrary in view of the errors generally associated with the experimental data. One alternative is to assume that a simple relation exists between the various phase shifts. While oversimplifying the situation, this assumption greatly reduces the number of parameters to be determined by experiment and allows an evaluation of the gross structure of the proton.

The results of the experiment to be described will be compared with the predictions of such a simplified optical model of the proton calculated according to the method of Fernbach, Serber, and Taylor.[1] Comparisons will also be made with the results of previous experiments.

[1] Fernbach, Serber, and Taylor, Phys. Rev. 75, 1352 (1949).

II. EXPERIMENTAL PROCEDURE

A. Exposure

A small stack of stripped, Ilford G-5, 600-micron emulsions was placed in a light-tight container on the end of a movable probe inside the vacuum tank of the Berkeley Bevatron. The geometry was such that when the probe was plunged into the beam, protons would enter through the edge, parallel to the plane of the emulsions. The stack was thus exposed to a pulse of approximately 10^7, 6.2-Bev protons. After the emulsions were developed, using standard techniques, it was found that this exposure resulted in an average of 4.7×10^5 beam protons/cm² in the region scanned.

B. Track Analysis

The plates were scanned using standard Bausch and Lomb, Leitz, Tiyoda, and Galileo binocular microscopes equipped with oil objectives and wide-field oculars with total magnifications of approximately 700X. All microscopes were equipped with a cross hair in one ocular which, when used in connection with an attached angular scale, allowed one to measure the projected angle between two tracks to within 0.5°. Dip angles were ascertained by measuring the change in depth of a track together with the corresponding projected track length. This change in depth was measured by taking advantage of the limited depth of field at large magnifications and a calibrated scale attached to the focusing adjustment of the microscope.

The space angles of the secondary protons were determined from the measured dip and projected angles by direct calculation, while the coplanarity of the three proton tracks was tested by plotting them on a 40-cm diameter stereographic projection calibrated in 1° intervals.

C. Preliminary Scanning

After attempting several scanning procedures, it was decided that the greatest number of proton-proton collisions was obtained by the method of secondary track scanning. Following this technique, one scans methodically through the emulsion, following all light tracks upstream to their origin. One may find by this

method an event of interest, a large nuclear star, or a point where the particle enters the emulsion. After recording this information as well as other data listed below, one returns to the point where the light secondary was originally intercepted and repeats the process.

Although this method yields a large number of proton-proton collisions, the inherent bias for locating various types of events must be ascertained so that their true, relative cross sections may be computed. To make this computation, the projected angle, ϕ, between the track followed and the incident proton, was recorded for every interaction located.

In order to increase statistics relating to the differential cross section of elastically scattered protons, area scanning was also employed. Although the scattered proton was rather difficult to detect in this fashion, the recoil proton, emerging at a large angle and with low energy, was easily seen. Since inelastic collisions were found only by secondary scanning, elastic events discovered by area scanning were not used to determine relative or absolute cross sections.

III. ANALYSIS OF $2p$ STARS

A. Selection Criteria

After the initial scan, $2p$ stars were relocated and examined with the following criteria in mind:

(a) The track of the incident proton must lie in the plane of the two secondaries.

(b) The angles of scattering, θ_1 and θ_2, are related by the expression

$$\tan\theta_1 \tan\theta_2 = 1 - (v/c)^2, \qquad (1)$$

where v is the velocity of the center-of-mass system with respect to the laboratory system.

(c) There must be no recoil blob, an indication of a collision with a bound proton.

Since quasi-elastic collisions as well as neutral meson production will destroy the uniqueness of criteria (a) and (b), a two-dimensional plot was made containing a point corresponding to each event, the two coordinates
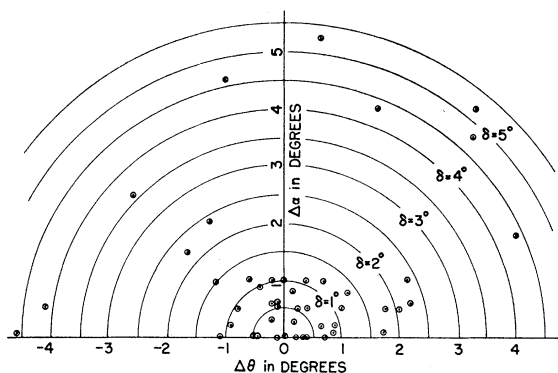
being measures of the degree to which these two criteria are not satisfied. This plot is shown in Fig. 1. One would expect a clustering of points about the origin with a spread due to errors in angle measurements, quasi-elastic events, neutral meson production, and background events. Specifically, the coordinates of Fig. 1 are

$$\Delta\theta = \tan^{-1}[(1 - v^2/c^2) \cot\theta_2] - \theta_1, \quad \Delta\theta \geqslant 0, \qquad (2)$$

and $\Delta\alpha$, which is equal to the magnitude of the angle between the incident track and the plane of the two secondaries. In order to analyze the plot of Fig. 1, a histogram was drawn showing the variation of the density of points on this plot as a function of the radial distance, δ, measured in degrees. This distribution is shown in Fig. 2, and is referred to, henceforth, as the δ distribution. Since the maximum of the δ distribution is rather broad, one must determine the range of δ values corresponding to free, elastic collisions. In order to do this, the distribution was decomposed by assuming that the contribution of quasi-elastic and background events varies slowly with δ. A straight-line extrapolation was then made to $\delta = 0$ from large δ. The area under this line represents the total number of quasi-elastic and background events in the range of δ shown.

Assuming that the portion of the δ distribution due to measurement errors can be represented by a Gaussian curve, several of these curves were drawn with various standard deviations, σ_δ, normalized so that the area from $\delta = 0$ to $\delta = \sigma_\delta$ is equal to the number of free elastic scatterings up to $\delta = \sigma_\delta$. A Gaussian was found which, when added to the quasi-elastic and background distribution, gives a good approximation to the experimental distribution of Fig. 2. The standard deviation of this curve is $\sigma_\delta = 1.5°$. Thus, in order to be accepted as elastic, an event is required to have $\delta \leq 1.5°$.

B. Scanning Efficiency

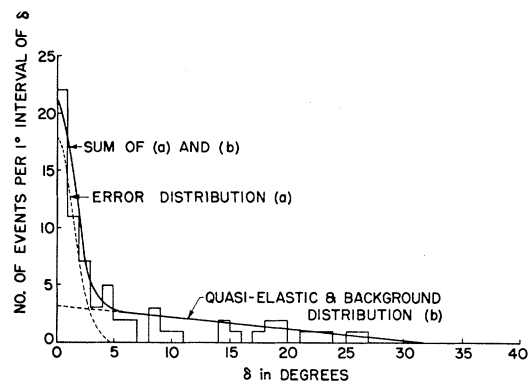One must also evaluate the effects of scanning efficiency on the relative number of the various elastic

FIG. 1. A plot of the angle of coplanarity, $\Delta\alpha$, vs the departure from angular correlation, $\Delta\theta$.

FIG. 2. A plot of the density of events, shown in Fig. 1, as a function of the radial distance, δ, from the origin of this figure. The solid and dotted curves are explained in the text.

TABLE I. Scanning efficiency as a function of projected scattering angle, ϕ.

ϕ, deg	0–2	2–4	4–6	6–8	8–10	10–12	12–14	14–16	16–18	18–20	20–22	22–24	24–26	26
$\epsilon(\phi)$	0.01	0.08	0.96	1.00	1.00	1.00	1.00	0.89	0.74	0.61	0.43	0.20	0.00	0.00

scattering final states discovered in scanning the plates. This was done by plotting the distribution of the projected angle, ϕ, for secondaries from large stars with dip angles, $\beta \leq 10°$, and grain densities, relative to the incident proton, $g \leq 1.2$. These restrictions are consistent with the criteria of the scanners in selecting light secondaries to follow back to their origin.

If one plots the distribution of secondaries followed to large stars in the course of the preliminary scan on the same graph, the two curves may be adjusted so that they are tangent to one another in a region where the scanning efficiency is believed to be close to unity, as shown in Fig. 3. The ratio of the ordinate of the lower curve to that of the upper curve, at any projected angle, ϕ, is the scanning efficiency at that angle. The total scanning efficiency, ϵ, is defined as

$$\epsilon = A'/A, \tag{3}$$

where A' is the area under curve (b) of Fig. 3 and A is the area under curve (a). Table I summarizes the partial scanning efficiencies, $\epsilon(\phi)$, determined from Fig. 3. The center-of-mass system angular distribution of elastically scattered secondaries may be then computed from the corrected number of elastic secondaries falling in the several ϕ intervals indicated in this table. Secondary protons from events detected by area scanning were added to the angular distribution without any correction for scanning efficiency, because of the ease with which the recoil protons could be detected.

C. Cross-Section Determination

The method of scanning used in this experiment does not directly yield a value for the absolute cross section for elastic scattering. However, since the secondaries followed during the scanning lead, most frequently, to large nuclear stars, it is possible to relate the cross section for elastic scattering to that for interation with nuclei of elements other than hydrogen. First, the total scanning efficiency, expression (3), was calculated for both elastic events ($\epsilon_e = 0.54$) and inelastic events ($\epsilon_s = 0.68$). Secondly, since only tracks making angles less than 10° with the surface of the emulsion were utilized in scanning, the average multiplicity, $\bar{n}$, of shower particles ($g \leqslant 1.2 \times \min$) was determined for this angular interval. This gave $\bar{n}_e = 1.00$ for elastic events in the forward direction and $\bar{n}_s = 1.10$ for inelastic ones. Next, the number of events, N, found by this method of scanning is given by

$$N_e \sim (\epsilon_e \bar{n}_e)/L_e \quad \text{and} \quad N_s \sim (\epsilon_s \bar{n}_s)/L_s, \tag{4}$$

for respectively elastic and inelastic events. The pro-

portionality constants are the same for both of the expressions (4) and L_e is the mean free path in emulsion for elastic events and L_s is that for inelastic ones. The mean value of L_s was computed[2,3] to be 36.4 cm, which can be used in (4) to find the mean path for elastic collisions.

IV. RESULTS

A. Cross Section

132 two-prong events were located by secondary scanning, of which 20 had $\delta \leq 1.5°$. Correction for scanning efficiency, ϵ_e, yields a total of 37 events. From an analysis of the δ distribution, 18.2% or 6.7 of these are quasi-elastic or background events, leaving a corrected total of 30.3 free, elastic events. The number of inelastic events found during the secondary scanning and corrected for scanning efficiency, ϵ_s, was 3063. Application of Eq. (4) then gives an elastic cross section of 8.8 ± 2.0 mb, the error being statistical only.

B. Angular Distribution

In addition to the 20 events mentioned in the last section, 11 elastic collisions were located by area scanning, giving a total of 31 acceptable events. The laboratory scattering angles, θ, of the secondaries from these events were transformed to the center-of-mass system by means of the relation

$$\tan\theta = (1 - v^2/c^2)^{\frac{1}{2}} \tan(\theta^*/2), \tag{5}$$

where θ^* is the scattering angle in the center-of-mass system and v is the velocity of the center-of-mass system with respect to the laboratory system.
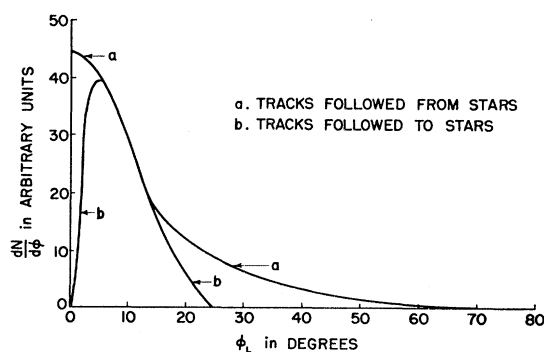

FIG. 3. A plot of the number of light secondaries from large, nuclear stars per unit interval of projected angle, ϕ, vs projected angle, ϕ.

[2] Cavanaugh, Haskin, and Schein, Phys. Rev. 100, 1263 (1955).
[3] G. Williams, Master's thesis, University of Washington, 1958 (unpublished).
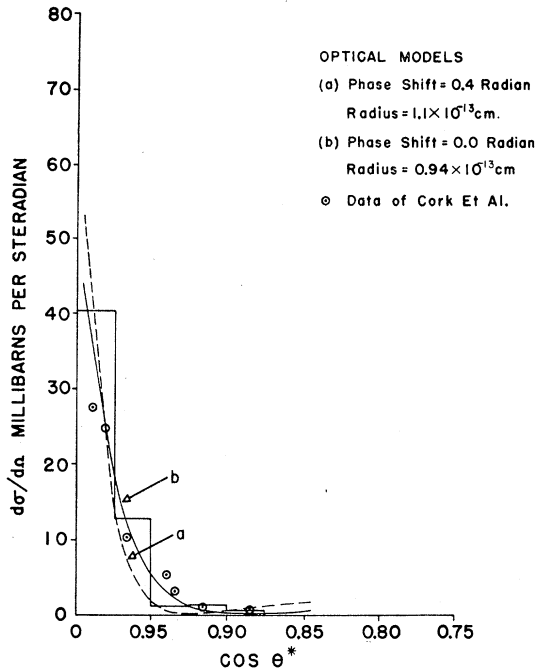
FIG. 4. A plot of the experimental, differential p-p elastic scattering cross section as a function of the cosine of the center-of-mass system scattering angle. The smooth curves are the results of two optical model calculations, mentioned in the text, and the circled points represent the data of Cork et al.[4]

Table II shows the uncorrected number of events per 0.025 interval of $\cos\theta^*$. The number listed for each interval is an average of the number of tracks in intervals of $\cos\theta^*$ which are symmetrically positioned about $\theta^* = 90°$. After correction for scanning efficiency, the number of events in each interval is multiplied by a normalizing factor so that the area of the resulting histogram is equal to the observed elastic cross section.
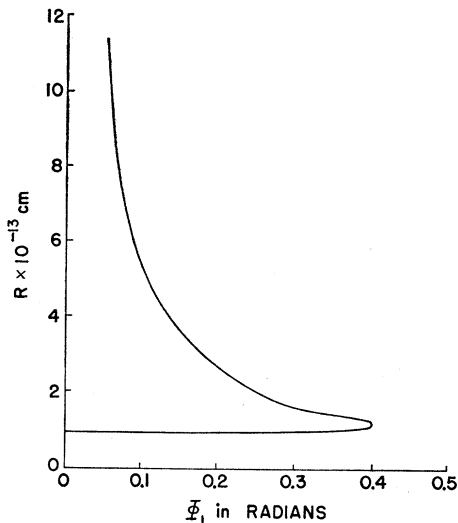

FIG. 5. A plot of the phase shift, Φ_1 as a function of the radius of interaction, R, for an elastic scattering cross section of 8.8 mb and an inelastic scattering cross section of 22.6 mb.

Table II also gives the corresponding differential cross sections and Fig. 4 shows the histogram.

C. Optical Model

In the absence of a complete theory, it has been customary to interpret the interactions of high-energy nucleons and mesons in terms of an optical model. The optical model changes the phase and amplitude of certain partial waves associated with the incident proton. This results in a diffraction scattering, while that part of the incident wave which is absorbed corresponds to inelastic scattering. If it is then assumed that incoherent elastic scattering is negligible, the elastic and inelastic scattering may be treated separately.

The parameters associated with an optical model are the radial variation of the density and the real and imaginary parts of the index of refraction. In the interest of simplicity, complications due to the spin and identity of the interacting particles are neglected, as are spin-orbit forces.

Since the data are meager, any number of such models could be formulated to fit the experimental results. However, it is of some interest to see whether the simple models formulated to explain elastic scattering at lower energies still give an adequate fit to the data at 6.2 Bev.

Such a model is a homogeneous disk of radius R. According to Fernbach, Serber, and Taylor,[1] the elastic cross section, σ_e, is given by

$$\sigma_e = 2\pi \int_0^\infty |1 - ae^{i\Phi}|^2 \rho d\rho, \qquad (6)$$

the inelastic cross section, σ_i, by

$$\sigma_i = 2\pi \int_0^\infty (1 - a^2)\rho d\rho, \qquad (7)$$

and the scattering amplitude by

$$f(\theta) = K \int_0^\infty |1 - ae^{i\Phi}| J_0(K\rho \sin\theta)\rho d\rho, \qquad (8)$$

where a is the amplitude and Φ is the phase of the transmitted wave whose initial amplitude and phase are unity and zero, respectively, ρ is the distance from the center of the interaction volume to the incident

TABLE II. Correction of angular distribution for scanning efficiency.

Range of $\cos\theta^*$	Uncorrected number of secondaries	Corrected cross section in millibarns per steradian
1.000–0.975	17.5	40.4
0.975–0.950	8.0	12.7
0.950–0.925	2.0	1.3
0.925–0.900	2.5	1.4
0.900–0.875	1.0	0.6
$0 \leqslant \cos\theta^* \leqslant 0.875$	0.0	0.0

particle in a plane perpendicular to its direction, and K is the propagation vector of the incident particle. The opacity, Θ, is often introduced in place of a, this quantity being defined by the relation

$$\Theta = 1 - a^2. \qquad (9)$$

For a homogeneous disk, we take $\Phi = \Phi_1$, $a = a_1$ for $\rho \leqslant R$, and $\Phi = 0$, $a = 1$ for $\rho > R$. Compatible values of σ_e, σ_i, Φ_1, a_1, and R are given by

$$\pi R^2 / \sigma_i = \{ \sin^2\Phi_1 + (\sigma_e/\sigma_i) \pm \cos\Phi_1 [(\sigma_e/\sigma_i)^2 \\ - \sin^2\Phi_1]^{\frac{1}{2}} \} / 2 \sin^2\Phi_1. \qquad (10)$$

The center-of-mass angular distributions of elastically scattered protons resulting from two optical models are compared with the results of the present experiment. Compatible values of the various parameters associated with a uniform optical model and the elastic and inelastic cross sections were obtained from Eq. (7) and Eq. (10). For the experimental elastic cross section of 8.8 mb and an inelastic cross section of 22.6 mb, Eq. (10) defines a relation between the phase shift, Φ_1, and the radius of interaction, R, which is shown in Fig. 5. Two extreme cases are examined: $\Phi_1 = 0.0$, $R = 0.94 \times 10^{-13}$ cm, $a_1 = 0.4$, and $\Phi_1 = 0.4$ radian, $R = 1.10 \times 10^{-13}$ cm, $a_1 = 0.64$. The angular distributions resulting from these two models are plotted in Fig. 4.

V. DISCUSSION

The observed cross section of 8.8 ± 2.0 mb is in general agreement with that which one would predict from the results at lower energies shown in Table III and also agrees with the value of 8 mb obtained by Cork and Wenzel[4] at 6.15 Bev, within experimental error. The differential cross sections obtained by these workers are plotted on Fig. 4 along with the data of the present

TABLE III. Elastic scattering cross-section measurements from 0.81 to 6.2 Bev.

Energy, Bev	Method	Cross section, mb	Reference
0.81	Cloud chamber	24 ± 2	Morris et al.[a]
0.925	Emulsion	17 ± 3	Duke et al.[b]
1.00	Counter	19 ± 3	Smith et al.[c]
1.50	Cloud chamber	20 ± 2	Fowler et al.[d]
2.24	Counter	17	Cork et al.[e]
2.75	Cloud chamber	15 ± 2	Block et al.[f]
3.00	Emulsion	8.9 ± 1.0	Cester et al.[g]
4.4	Counter	10	Cork et al.[e]
5.7	Emulsion	13 ± 6	Giles[h]
6.15	Counter	8	Cork et al.[e]
6.2	Emulsion	8.8 ± 2.8	Present experiment

[a] Morris, Fowler, and Garrison, Phys. Rev. 103, 1472 (1956).
[b] Duke, Lock, March, Gibson, McEwen, Hughes, and Muirhead, Phil. Mag. 2, 204 (1957).
[c] Smith, McReynolds, and Snow, Phys. Rev. 97, 1186 (1955).
[d] Fowler, Shutt, Thorndike, and Whittemore, Phys. Rev. 103, 1479 (1956).
[e] See reference 4.
[f] Block, Harth, Cocconi, Hart, Fowler, Shutt, Thorndike, and Whittemore, Phys. Rev. 103, 1484 (1956).
[g] Cester, Hoang, and Kernan, Phys. Rev. 103, 1443 (1956).
[h] P. C. Giles, University of California Radiation Laboratory Report UCRL-3223 (unpublished), p. 12.

[4] Cork, Wenzel, and Causey, Phys. Rev. 107, 859 (1957).

TABLE IV. Uniform optical models calculated for proton-proton elastic scattering at various energies.

Energy, Bev	Opacity	Radius (cm)	Reference
0.810	0.97	0.93×10^{-13}	Fowler et al.[a]
0.925	$\cdots$	0.9×10^{-13}	Duke et al.[b]
1.50	0.96	0.93×10^{-13}	Fowler et al.[a]
2.75	0.92	0.93×10^{-13}	Fowler et al.[a]
3.0	1.00	1.0×10^{-13}	Cester et al.[c]
6.2	0.81	0.94×10^{-13}	Present experiment

[a] Fowler, Shutt, Thorndike, Whittemore, Cocconi, Hart, Block, Harth, Fowler, Garrison, and Morris, Phys. Rev. 103, 1489 (1956).
[b] Duke, Lock, March, Gibson, McEwen, Hughes, and Muirhead, Phil. Mag. 2, 204 (1957).
[c] Cester, Hoang, and Kernan, Phys. Rev. 103, 1443 (1956).

experiment. Principal disagreement occurs at small angles where counter experiments are difficult because of the proximity of one counter to the proton beam. On the other hand, the emulsion results are quite sensitive to scanning efficiency in this region.

Knowledge of the elastic and inelastic cross section permits one to formulate a group of uniform optical models. For any model of this group, however, the radius and phase shift must be related according to Eq. (10). This expression also defines a range of Φ_1 values which are compatible with the observed cross sections, the range for the present experiment being

$$0 \leqslant \Phi_1 \leqslant 0.4 \text{ radian.}$$

When the differential cross sections resulting from models with acceptable phase shifts are compared with the results of the present experiment, it appears that closest agreement is obtained for $\Phi_1 = 0$. This value of Φ_1 also corresponds to the minimum value of R which is compatible with the experimental data. The model which gives closest agreement with the observed differential cross section has the parameters

$$R = 0.94 \times 10^{-13} \text{ cm}, \quad \Phi_1 = 0.00 \text{ radian},$$

$$a_1 = 0.44 \quad (\text{opacity} = 0.81).$$

Table IV lists a number of uniform optical models formulated to fit elastic scattering data at lower energies. Considering experimental uncertainties, it would appear that a single optical model could be defined which would give agreement over the entire energy range of 0.81–6.2 Bev. However, until more precise total and differential cross sections are obtained, the energy dependence of the parameters of these simple optical models will remain somewhat uncertain.

ACKNOWLEDGMENTS